Statistical simultaneous multifragmentation model for heavy ion collisions with entrance channel characteristics

C. B. Das, A. Das, and L. Satpathy
Institute of Physics, Bhubaneswar 751 005, India

M. Satpathy
Department of Physics, Utkal University, Bhubaneswar 751 004, India
(Received 17 November 1995)

Based on the fireball model and the spectator-participant picture, a statistical simultaneous multifragmentation model is developed for heavy ion induced reactions, with the entrance channel characteristics taken into account. This model has the density as the only parameter and it predicts the excitation energy, the temperature, and the frgmentation cross section, etc., once the incident energy, the projectile, and the target nuclei are specified. As a first application, it has been applied to the central collision data taken at National Superconducting Cyclotron Laboratory on the $^{40}Ar+^{45}Sc$ reaction at incident energies ranging from 35 to 115 MeV/A. The study brings out the similarity in the characteristics of high energy proton induced and medium energy heavy ion induced reactions. It is observed that with rise of bombarding energy, the onset of simultaneous multifragmentation occurs at some energy between 50 and 60 MeV/A.

PACS number(s): 25.70.Pq, 24.10.Pa

I. INTRODUCTION

A heavy nucleus undergoes binary decay in the well known fission process, when a thermal neutron of almost negligible energy strikes it. However, when a very high energy proton or a mediun energy heavy ion collides with a target nucleus imparting several hundred MeV of energy, it decays into many fragments. Whether this process is a series of sequential binary decays or a simultaneus decay to many fragments, which is a completely new mode of decay of the nucleus, has been an important question in recent years. It has not yet been possible to satisfactorily resolve it at the experimental level. In the scenario emerging from many model studies [1–3], there has been indication that at lower bombarding energy, the former mechanism prevails, and at higher bombarding energies, the latter dominates. However, the true nature of the mechanism, excitation energy, temperature, etc. of this decay are yet to be ascertained fully.

Another major interest in the phenomena of multifragmentation has been the possibility of observation of a liquid-gas phase transition in nuclear systems. The liquidlike behavior of finite nuclei in the ground state has been recognized since the early days of nuclear physics. Since the advent of heavy ion collision, it has been possible to heat the nucleus and study the extent of temperature up to which this property persists to see if eventually one could find the liquid-gas phase transition. It is expected that a process like multifragmentation, through which a hot nucleus decays, is likely to carry this signature. The earliest effort in this regard has been the Fermilab-Purdue experiment on $p+\mathrm{Kr}$ and $p+\mathrm{Xe}$ reactions in which the mass yield was fitted with the power law A^{τ} prescribed by the Fisher droplet model [4]. However, an alternative description of the same data through models which do not explicitly have a liquid-gas phase transition mechanism [5–8] rendered this matter inconclusive. Since then, other investigations have been carried out, but it has not been possible to arrive at a definite conclusion.

It must be emphasized that multifragmentation phenomena offer the possibility of production and study of low density nuclear matter in the laboratory, which is of equally great astrophysical importance as high density nuclear matter.

In heavy ion collisions, the excitation energy imparted to the composite system before the fragments are emitted is the key variable which governs the nature of the decay process. To identify various processes operative at different regimes of energy, it is worthwhile to develope good and precise models based on definite mechanisms. In this regard, we have attempted to build a simultaneous multifragmentation model appropriate for collision of two heavy ions at intermediate energies with the specific aim of finding the bombarding energy, excitation energy, temperature, and density at which this process is favored. In the past, we have developed a statistical simultaneous multifragmentation model for high energy proton induced heavy ion collisions using the grand canonical picture, taking into account both the nuclear and Coulomb fragment-fragment interactions [9] through the respective mean fields calculated using a well defined statistical procedure. The success of this improved statistical model has been amply demonstrated [9–11] through the enhancement of neutron and other charge particle multiplicities, reduction of temperature, and simultaneous description of mass yield, isotopic yield, and kinetic energy spectra. This was an extension of our earlier model proposed in collaboration with Gross *et al.* in which only Coulomb interaction was taken into account, treating the Coulomb radius as an extra parameter [12]. One major deficiency of such models is that the incident energy did not specifically enter into the calculation and the excitation energy could not be specified. It could be estimated from the temperature, which was treated as a parameter in the model, determined from the fit to mass yield and other data. In the present work, we attempt to develop a statistical simultaneous multifragmentation model in which this drawback is removed and the entrance channel characteristics are taken into account. The model has

only one parameter, namely, the density of the decaying system, and it gives an estimate of the excitation energy, mass yield, and temperature, etc., once the bombarding energy, projectile, and target nuclei are specified.

The general features of collisions between two complex nuclei for bombarding energy below 10 MeV/A show strong collective behavior of matter in bulk, which is manifested in phenomena like deep inelastic collision, fusion, fission, quasielastic processes etc. At high relativistic energies, the collision process is dominated by the interaction of the individual nucleons in the projectile with their counterparts in the target. For such an energy regime, the fireball model and the spectator-participant picture [13], in which the tripartition of the total system takes place, have been quite successful. For the intermediate energy range of 20 to 200 MeV one expects a drastic change of the mechanism in the nuclear collision, as it includes the landmark Fermi energy of 35 MeV for the nuclear matter, which determines the nature of the response of the nucleus to external perturbation. For energies around and above the Fermi energy, the nucleus no longer responds as a whole to the collision. Thus the fireball model has been found very useful for the description of intermediate energy heavy ion collisions. Such a picture has been used to describe data obtained with energy 20 MeV/A, even as low as 13 MeV/A [14,15]. Hence we adopt such a framework in developing our statistical simultaneous multifragmentation model.

An outline of the model is presented in Sec. II. In Sec. III we apply this model to the specific case of the central collision data taken at Michigan State University on the ^{40}Ar induced ^{45}Sc reaction with incident energy varying from 35 to 115 MeV per nucleon. The results and discussion are presented in Sec. IV. Finally in Sec. V we conclude.

II. THE MODEL

Consider a heavy nucleus with mass number A_T at rest in the laboratory undergoing collision at a given impact parameter with a projectile nucleus having mass number A_P and energy $E^P_{\rm lab}$. Assuming the fireball model and the spectator-participant picture [13] for the collision process, one would expect contributions to the fragmentation yield from three sources, namely the fireball formed by the participant parts, and the projectilelike and targetlike spectator parts. The projectilelike spectator moves in the laboratory with a longitudinal velocity the same as the velocity of the projectile, while the targetlike part remains at rest. For calculation of the fragmentation cross section we have to know the excitation energies and the constitution of each part. In this model the number of nucleons constituting each part is determined from the geometry.

A. Determination of constitution and the excitation energy

1. Fireball part

For a given impact parameter b, say, $A_{P'}$ and $A_{T'}$ nucleons are severed from the projectile and the target respectively and form the fireball. For the calculation of these numbers, the prescription given in Ref. [13] is followed. We adopt relativistic kinematics for the calculation of excitation energy.

The lab energy of the projectile and the target part which forms the fireball are given by

$$E^P_{\rm lab}=A_{P'}\times(\epsilon+m'), \tag{1}$$

$$E^T_{\rm lab}=A_{T'}\times m', \tag{2}$$

where ϵ is the lab energy per nucleon of the projectile, m' is the effective nucleon mass in the nuclei, i.e., 931 MeV, and $A_{P'}$ and $A_{T'}$ are the number of nucleons from the projectile and the target, respectively, that form the fireball. Then we have the momentum of the projectile in the laboratory frame,

$$P^P_{\rm lab}=\sqrt{(E^P_{\rm lab})^2-(m'A_{P'})^2}. \tag{3}$$

So the center of mass energies of the two parts are given by

$$E^P_{\rm c.m.}=\gamma\times(E^P_{\rm lab}-\beta P^P_{\rm lab}) \tag{4}$$

$$E^T_{\rm c.m.}=\gamma\times E^T_{\rm lab}, \tag{5}$$

where $\gamma=1/\sqrt{1-\beta^2}$, and β is given by

$$\beta=\frac{P^P_{\rm lab}}{(E^P_{\rm lab}+E^T_{\rm lab})} \tag{6}$$

So the excitation energy in the c.m. frame is

$$E^\star=E_{\rm c.m.}-m\times(A_{P'}+A_{T'}), \tag{7}$$

m being the free nucleon mass (=939 MeV) and $E_{\rm c.m.}$ the total center of mass energy, $E^P_{\rm c.m.}+E^T_{\rm c.m.}$

2. Projectilelike spectator part

The projectilelike spectator (PS) part will be moving with the same velocity as that of the projectile before the collision in the laboratory. Being severed, this part will have $(A_P-A_{P'})$ number of nucleons, and due to distortion, will be in an excited state of the corresponding nucleus with the same nucleon number. The excitation energy can be estimated by calculating the change in the surface energy ΔE_s and the Coulomb energy ΔE_c from that of the spherical shape appropriate for the ground state. The calculation of ΔE_s and ΔE_c is done following the prescription described in the Appendix. Then the excitation energy for the projectilelike spectator part in its frame is given by

$$E^*_P=\Delta E_s+\Delta E_c\,. \tag{8}$$

3. Targetlike spectator part

The excitation energy of the targetlike spectator (TS) part, E^*_T, will be determined exactly like the projectilelike spectator part. However, this energy will be in the rest frame of the target.

After determining the number of constituent nucleons and the excitation energy of all the three parts, we study their fragmentation following the mechanism described below.

B. Statistical decay of the excited system

The three parts described above have specified amounts of excitation energy, due to which each will undergo decay into various fragments, which in a statistical model will be governed by the available phase space. For the decay of each part, we follow the basis of the grand canonical model developed earlier [9–12]. The important difference here is that we describe the collision between two heavy ions with the energy being specified *a priori* in the present case, while it was an unknown quantity in the former case.

We consider an assembly of fragments at statistical equilibrium with temperature T, interacting through both the nuclear and Coulomb interactions. In this model, the logarithm of the grand partition function ξ, in terms of neutron and proton chemical potentials μ_n and μ_p and the inverse temperature $\beta=1/\kappa T$, is obtained as

$$\ln\xi(\mu_n,\mu_p,\beta)=\sum_i w_i(\mu_n,\mu_p,\beta), \tag{9}$$

where w_i is the multiplicity of a particular fragment of type i.

The expression for $w_i(\mu_n,\mu_p,\beta)$ is given by

$$w_i(\mu_n,\mu_p,\beta)=\left(\frac{MA_i}{2\pi\hbar^2\beta}\right)^{3/2} V\phi_i(\beta)\times\exp\{-\beta[-B_i+\bar{C}_i+\bar{V}_i-\mu_n(A_i-Z_i)-\mu_p Z_i]\}. \tag{10}$$

Here $V=4\pi r_0^3 A/3$ is the volume of the expanded fireball with r_0 being the radius constant, related to the freeze-out density. B_i is the binding energy, and ϕ_i (β) is the internal partition function of the excited but particle-stable states of fragment i. $\bar{C}_i$ and $\bar{V}_i$ are the mean Coulomb and nuclear interaction of the fragment i with the rest of the system.

Knowing the excitation energy $E^\star$, the charge number Z, and the baryon number A of the decaying system, one has to solve the following three conservation equations, to get consistent values for the three unknown quantities μ_n, μ_p, and T:

$$A=\sum_i A_i w_i(\mu_n,\mu_p,\beta), \tag{11}$$

$$Z=\sum_i Z_i w_i(\mu_n,\mu_p,\beta), \tag{12}$$

$$E^\star=-\frac{\partial}{\partial\beta}\ln\xi(\mu_n\mu_p,\beta), \tag{13}$$

where A_i and Z_i are the mass and charge number of the fragment of type i.

Getting all three quantities μ_n, μ_p, and T, we have the mean multiplicity $\langle n_i(b)\rangle$ of a fragment of type i, for particular impact parameter b, given as

$$\langle n_i(b)\rangle=w_i(\mu_n,\mu_p,\beta). \tag{14}$$

Hence the cross section σ_i for the production of fragment i at some b in a nucleus-nucleus collision is given by

$$\sigma_i=\langle n_i(b)\rangle\sigma_{\rm in} \tag{15}$$

where $\sigma_{\rm in}$ is the total inelastic cross section.

To get the cross section for all impact parameters one has to integrate it over all b's:

$$\sigma_i=\int n_i(b)2\pi b\,db. \tag{16}$$

Finally one has to take the contributions to the cross section from all the three parts, converted to the c.m. frame, and add them up to get the total yield:

$$\sigma_{\rm total}=\sigma_{\rm FB}+\sigma_{\rm PS}+\sigma_{\rm TS}. \tag{17}$$

III. APPLICATION TO CENTRAL COLLISION PROCESS

As a first application, we apply the model to the case of central collision of two nuclei having nearly equal numbers of nucleons. In particular, we attempt to explain the central collision data of the ^{40}Ar induced reaction on ^{45}Sc taken at the National Superconducting Cyclotron Laboratory of Michigan State University (MSU), with incident energy varying from 35 MeV/A to 115 MeV/A [16]. Since we have collision between two systems having almost equal numbers of nucleons, we restrict our calculation to the fireball part only, which has $A=80$ and $Z=36$. The contribution from the targetlike spectator part to the total yield is very small, and can be neglected.

Determinimg A, Z, and $E^\star$, we solve the three conservation Eqs. (11)–(13) to get μ_n, μ_p, and T consistently. Using those values we obtain w_i and hence $\langle n_i(0)\rangle$. For $\sigma_{\rm in}$ we take the empirical parametrization

$$\sigma_{\rm in}=\pi R_0^2\times[(A_p^{1/3}+A_T^{1/3})-b_0(A_p^{-1/3}+A_T^{-1/3})]^2 \tag{18}$$

used by Heckman *et al.*, [17] where $R_0=1.36$, $b_0=0.75$, and A_p and A_T are the mass numbers of projectile and target nuclei.

In our calculation of the mean nuclear interaction $\bar{V}_i$, we have followed the statistical prescription developed earlier [9,10]. We have used the proximity potential for the heavy fragments and the actual optical potentials for the lighter ones. We have taken the value of r_0 to be 1.85 fm which corresponds to a freeze-out density $0.22\rho_0$ for which we got

TABLE I. Excitation energy per nucleon and temperature of the excited system at different bombarding energies (all quantities are in MeV).

Bombarding energy per nucleon	Excitation energy per nucleon	Temperature
35	0.7091	2.3358
45	3.1828	4.5755
65	8.1105	6.5895
75	10.5648	7.7300
85	13.0129	8.8301
95	15.4545	9.8861
105	17.8899	10.9036
115	20.3194	11.8872

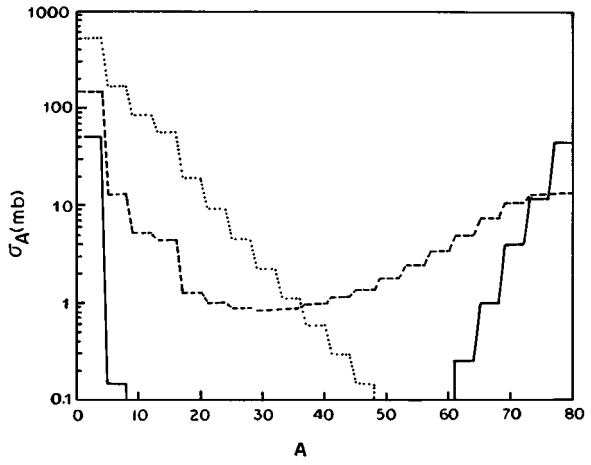

FIG. 1. Mass distributions for central collision of ^{40}Ar+^{45}Sc at different lab energies. The solid, dashed, and dotted lines are for lab energies 35, 40, and 65 MeV/A, which correspond to temperatures 2.33, 3.90, and 6.59 MeV, respectively.

the best fit with the experimental data, where $\rho_0 = 0.17$ fm^{-3} is the nuclear matter ground state density.

First we would like to make a model study to see if the general features of mass yield, like the **U** shape, and exponentially falling shape, etc., seen in high energy proton induced nucleus collision which could be described in our previous model, are also reproduced in the present case where temperature is no longer a parameter. Taking $E_{\rm lab} = 35$, 40, and 65 MeV/A for the present reaction ^{40}Ar + ^{45}Sc we obtained $T = 2.33$, 3.90, and 6.59 MeV, for which the mass yields are shown in Fig. 1. We find that the shoulderlike, **U** shape, and exponentially falling shape of distributions for low $T = 2.33$ MeV, medium $T = 3.90$ MeV, and high $T = 6.59$ MeV, respectively, are reproduced in the same temperature regimes as in the case of proton induced reactions. So it is satisfying to find that introduction of new elements like the bombarding energy dependence and heavy ions as projectiles yields similar general features. This further brings out the similarity between the dynamics of high energy proton induced multifragmentation processes and intermediate energy heavy ion reactions. This enhances our confidence about the suitability of the present model for the description of the MSU data.

IV. RESULTS AND DISCUSSIONS

We would like to emphasize at this stage that except the value of r_0 which determines the density, the present model has no other parameter. The Coulomb and nuclear mean fields are also totally fixed by this parameter. We have carried out calculations for all the eight sets of data obtained with bombarding energy ranging between 35 MeV/A and 115 MeV/A. The corresponding excitation energies and temperatures obtained in our study are summarized in Table I. It is interesting to note that the values of the temperatures lie in the appropriate range where multifragmentation phenomena have been observed in high energy proton induced heavy ion reactions. In Fig. 2, we have presented the cross sections as a function of fragment charge as open circles, and compared with the experimental data [16], given as filled circles and the histogram, which are corrected and uncorrected for acceptance, respectively. It can be seen that the general trend of the steepness of the charge distribution with increasing energy is quite well reproduced for all the beam energies higher than 45 MeV/A, where as for 35 MeV/A it is quite poor. In Figs. 3 and 4, we have presented the average number of

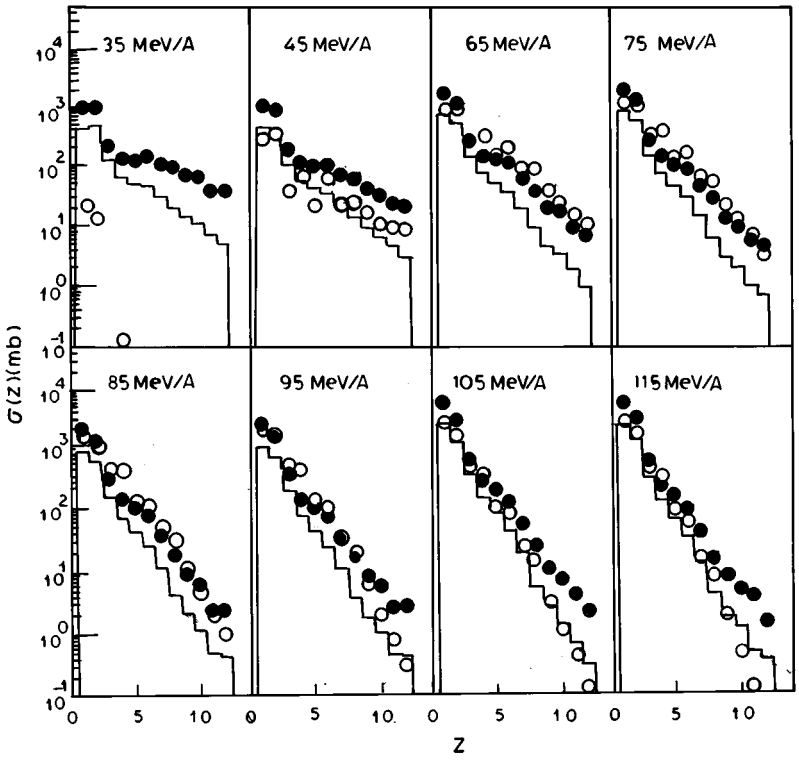

FIG. 2. Charge distribution for central collision of ^{40}Ar+^{45}Sc. The open circles are the results obtained in the present model. The histogram and the solid circles represent the uncorrected and the corrected data for the reaction ^{40}Ar+^{45}Sc taken from Ref. [13].

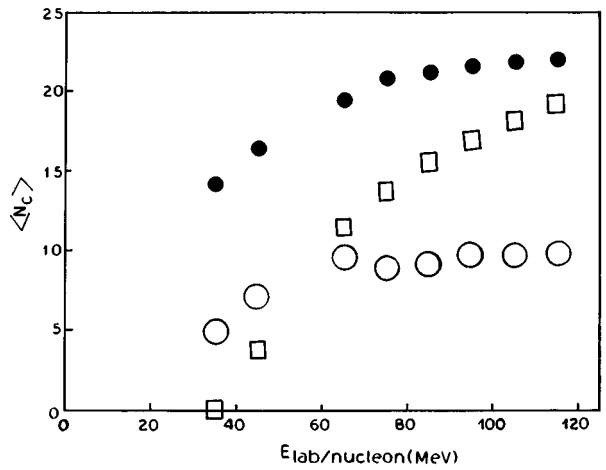

FIG. 3. The average number of charge particles $\langle N_c \rangle$ plotted against incident beam energy. The open and the solid circles represent the uncorrected and the corrected data for the reaction ^{40}Ar+^{45}Sc taken from Ref. [13] and the squares represent the results of the present study.

charge multiplicity $\langle N_c \rangle$, and the average number of intermediate mass fragments $\langle N_{\rm imf} \rangle$, by squares. We have confined the Z value to lie in the range $1 \leqslant Z \leqslant 12$ for calculation of $\langle N_c \rangle$, and $3 \leqslant Z \leqslant 12$ for $\langle N_{\rm imf} \rangle$, to compare with the data measured with such restrictions [16]. The filled and open circles are, respectively, the corrected and uncorrected data for acceptance. It can be seen that our charge multiplicity increases and the $\langle N_{\rm imf} \rangle$ decreases with increasing beam energy, in agreement with the experimental trend. However, for both these cases, our result is rather poor for the beam energies 35 and 45 MeV/A. Thus the comparison of our results for these three sets of data clearly points out that the model is quite successful for all the higher bombarding energies commencing from 65 MeV/A.

To get a comprehensive understanding of the observed data, we have calculated the cross section for fragments with

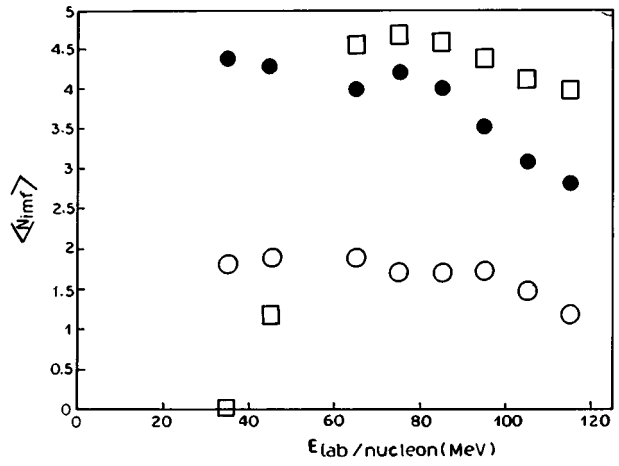

FIG. 4. The average number of intermediate mass fragments $\langle N_{\rm IMF} \rangle$ plotted against incident beam energy. The symbols have the same meaning as in Fig. 3.

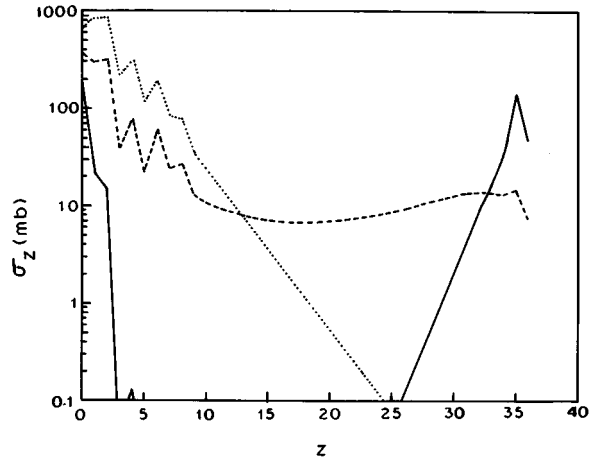

FIG. 5. Total charge distribution for central collision of ^{40}Ar+^{45}Sc at different lab energies. The solid, dashed, and dotted lines are for lab energies 35, 45, and 65 MeV/A, which correspond to temperatures 2.33, 4.57, and 6.59 MeV.

all possible Z values extending up to 36 for three different beam energies and plotted them in Fig. 5. The solid, dashed, and dotted lines represent the cross sections for beam energies 35, 45, and 65 MeV/A, respectively. For the case of $E_{\rm lab}=65$ MeV/A the yield for fragments with charge number greater than 12 falls very sharply and beyond charge number 25 it is less than 0.1 mb. For the case of $E_{\rm lab}=45$ MeV/A our calculation shows a flat distribution of charge covering up to $Z=36$ although somewhat lower in magnitude compared to the observed ones up to $Z=12$. Extending the observations for intermediate charge fragments, one would find a sizable yield as per this calculation. However, in the experiment only a part of it has been observed. This case is reminiscent of the U shape of mass yield. Thus 45 MeV/A corresponding to temperature 4.57 MeV marks a transition point, above which exponential-like decay of charge distribution is favored. For beam energy 35 MeV/A, we have two branches in the charge yield with Z less than 5 and more than 25. This distribution has no resemblance to the observed yield. This seems to point to the fact that with such a low excitation energy the system does not decay through the mechanism of simultaneous multifragmentation but rather by some other mechanism. To arrive at a general picture, we have plotted the temperature versus the beam energy in Fig. 6. We find that the curve shows strong linear behavior for higher energies, commencing around beam energies 50 to 60 MeV/A. Thus, taking this fact into account, together with the quality of our results shown in Figs. 2, 3 and 4, it is reasonable to interpret that the system decays by simultaneous multifragmentation processes above the beam energy $\sim$60 MeV/A, and below it by some other process, maybe that of binary sequential decay. The present result does not change appreciably when we take a fully fused system having $A=80$ and $Z=39$ as the fireball. It is gratifying to find that Cebra *et al.* [1] and Barz *et al.* [2] have also observed from their event-shape analysis of central collision data of ^{40}Ar + ^{51}V that at 35 MeV/A the decay is sequential in nature and the onset of simultaneous multifragmentation decay occurs between 45 and 65 MeV/A. This is also in accord with Trockel *et al.* [3], who have

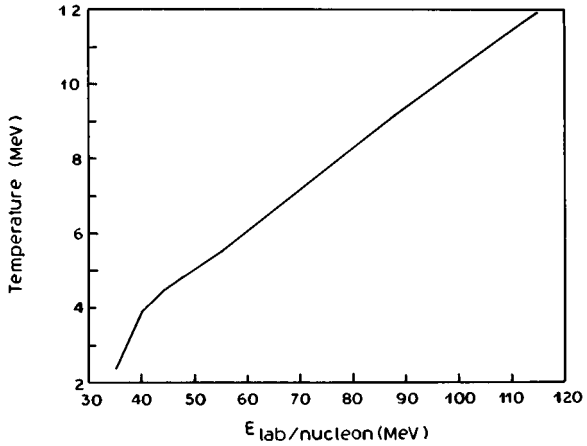

FIG. 6. The variation of temperature of the excited system with incident beam energy.

also observed from their analysis of reactions of ^{12}C, ^{18}O, ^{20}Ne, and ^{40}Ar on ^{nat}Ag and ^{197}Au, that the onset of multifragmentation occurs at excitation energy 300 MeV, which corresponds to lab energy of 48 MeV/A for our system. The present study clearly shows that the three sets of data, namely, the charge yield, the average number of charged particles and average number of intermediate mass fragments as a function of incident energy, can be described for all energies at and above 65 MeV/A. Thus it is reasonable to conclude that onset of simultaneous multifragmentation might take place in the energy range 45 to 65 MeV/A.

The above MSU data have also been fitted by Li *et al.* [16] to a power law A_f^{τ} predicted in the Fisher droplet model. Combining with previous results, they find a minimum in the value of τ as a function of bombarding energy at 35 to 50 MeV/A beam energy regime. They suggest that this minimum might be related to a liquid-gas phase transition occurring around that energy. As shown above, we find in this energy regime that the **U** shape occurs in the mass yield, which evolves to an exponential-like fall when the bombarding energy is increased. Since below this energy regime, the mechanism of simultaneous multifragmentation cannot describe the data, while that of sequential binary can account for them, it is very likely that this energy region marks a transition at which the mechanism of decay changes from sequential to a simultaneous multifragmentation process. Recently Pan and Das Gupta [18] have also found the signature of a phase transition in a similar energy regime in a lattice gas model. Whether all these transitions are related at a fundamental level is an important question which needs further work for a clear answer.

V. CONCLUSIONS

In summary, we have developed a statistical simultaneous multifragmentation model for the collision of two heavy ions, based on the fireball model and spectator-participant picture, taking into account the entrance channel characteristics. Given the incident energy and the projectile and target nuclei, the model predicts the excitation energy, temperature, and fragmentation cross section without any adjustable free parameter except the density. The drawback of treating temperature as a parameter, previously resorted to in the description of proton induced heavy ion collisions has been successfully removed. The present study shows that the general features of multifragmentation processes encountered in high energy proton induced reactions and intermediate energy heavy ion induced reactions are similar in nature. As a first application we have attempted to describe the recent MSU data on ^{40}Ar+^{45}Sc for central collision at incident energies ranging from 35 to 115 MeV/A. The model can satisfactorily describe the charge yield, the average number of charge particles, and the average number of intermediate mass fragments for incident energies 65 MeV/A and above. The study gives the freeze-out density to be 0.22 times the nuclear matter density. The present study suggests that the critical point at which the onset of simultaneous multifragmentation occurs lies somewhere in the range 50 to 60 MeV/A. Also there have been speculations that the liquid-gas phase transition in nuclear matter may occur in this energy range. However, more work is necessary to establish this phase transition in nuclear systems and to see if it is related to the onset of multifragmentation processes. Application of this present

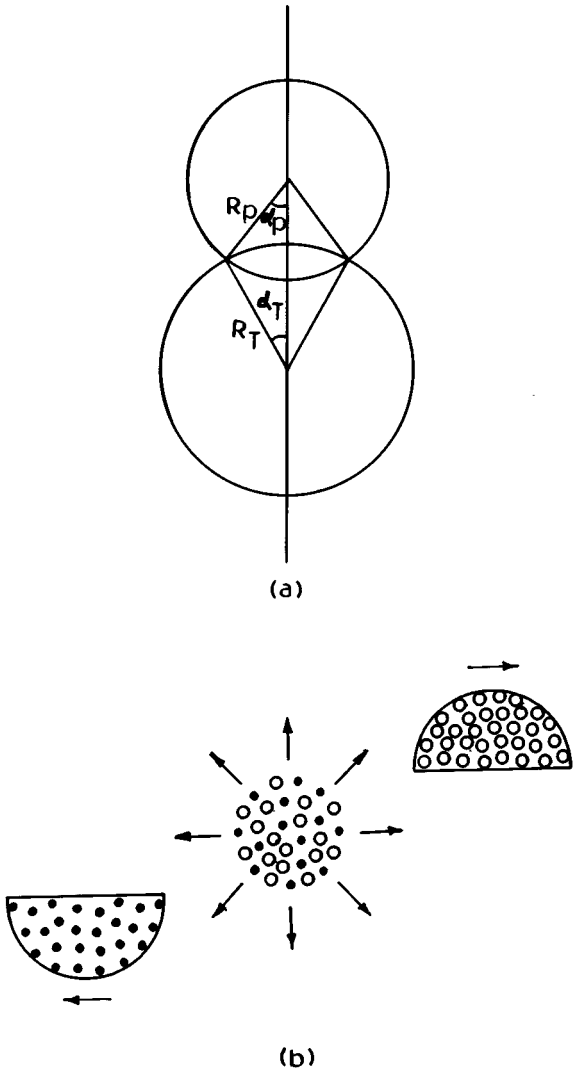

FIG. 7. Schematic diagram showing the geometry during and after the collision process in (a) and (b) respectively.

model to a more general case of noncentral collisions will appear elsewhere.

ACKNOWLEDGMENT

One of the authors (A.D.) acknowledges the assistance provided by CSIR for the present work.

APPENDIX

To calculate the change in the surface and Coulomb energies, ΔE_s and ΔE_c respectively, of the projectilelike and the targetlike spectators, we consider the general case of impact parameter b in the range $R_T-R_P<b<R_T+R_P$, where R_T and R_P are the radii of the target and the projectile nuclei, respectively. The schematic picture showing the geometry during the collision and after collision for a given impact parameter is shown in Figs. 7(a) and 7(b). The projectilelike spectator PS and the targetlike spectator TS will have mass numbers $(A_P-A_{P'})$ and $(A_T-A_{T'})$, where $A_{P'}$ and $A_{T'}$ are the severed parts forming the fireball. The values of $A_{P'}$ and $A_{T'}$ are determined following Appendix 4 of Ref. [13].

From simple geometrical analysis we have the surface area of the projectilelike and the targetlike spectators ($S_{\rm PS}$ and $S_{\rm TS}$, respectively) as given by

$$S_{\rm PS}=2\pi r_0^2 A_P^{2/3}(1+\cos\alpha_P)+\pi r_0^2 A_P^{2/3}(1-\cos^2\alpha_P), \quad \text{(A1)}$$

$$S_{\rm TS}=2\pi r_0^2 A_T^{2/3}(1+\cos\alpha_T)+\pi r_0^2 A_T^{2/3}(1-\cos^2\alpha_T), \quad \text{(A2)}$$

where α_P and α_T are defined in the figure. In terms of the impact parameter b these two angles are given as

$$\cos\alpha_P=\frac{b^2+r_0^2(A_P^{2/3}-A_T^{2/3})}{2br_0A_P^{1/3}} \quad \text{(A3)}$$

$$\cos\alpha_T=\frac{b^2+r_0^2(A_T^{2/3}-A_P^{2/3})}{2br_0A_T^{1/3}}. \quad \text{(A4)}$$

The corresponding surface area of the projectilelike part in its spherical ground state, denoted by $S^0_{\rm PS}$, is given as

$$S^0_{\rm PS}=4\pi r_0^2(A_P-A_{P'})^{2/3}. \quad \text{(A5)}$$

So we have the change in the surface energy for the projectilelike part,

$$\Delta E_s=(S^0_{\rm PS}-S_{\rm PS})\sigma \quad \text{(A6)}$$

where σ is the surface energy coefficient.

The Coulomb energy of the projectilelike part $E_{c\rm PS}$ in its distorted shape is given by

$$E_{c\rm PS}=\frac{1}{2}\int\int\frac{\rho(r)\rho(r')}{|r-r'|}d^3r\,d^3r' \quad \text{(A7)}$$

where $\rho(r)$ and $\rho(r')$ are the charge distributions in two different infinitesimal volume elements d^3r and d^3r', respectively, and the integration is carried over the entire distorted volume, which has to be calculated numerically.

The Coulomb energy of this part in its spherical ground state ($E^0_{c\rm PS}$) is

$$E^0_{c\rm PS}=\frac{3Z^2e^2}{5r_0(A_P-A_{P'})^{1/3}}. \quad \text{(A8)}$$

So the change in the Coulomb energy for the projectilelike part is given by

$$\Delta Ec=E^0_{c\rm PS}-E_{c\rm PS}. \quad \text{(A9)}$$

For the targetlike part both ΔE_s and ΔE_c have similar expressions.

[1] D. A. Cebra, S. Howden, J. Karn, A. Nadasen, C. A. Ogilvie, A. Vander Molen, G. D. Westfall, W. K. Wilson, J. S. Winfield, and E. Norbeck, Phys. Rev. Lett. **64**, 2246 (1990).

[2] H. W. Barz, D. A. Cebra, H. Schulz, and G. D. Westfall, Phys. Lett. B **267**, 317 (1991).

[3] R. Trockel, K. D. Hildenbrand, U. Lynen, W. F. J. Müller, H. J. Rabe, H. Sann, H. Stelzer, W. Trautmann, R. Wada, E. Eckert, P. Kreutz, A. Kühmichel, and J. Pochodzalla, Phys. Rev. C **39**, 729 (1989).

[4] M. E. Fisher, Physics **3**, 255 (1967); Rep. Prog. Phys. **30**, 615 (1967).

[5] J. P. Bondorf, Nucl. Phys. **A387**, 250 (1982).

[6] J. Hüfner, Phys. Rep. **125**, 129 (1985).

[7] X. Campi, J. Desbois, and E. Lipparini, Phys. Lett. B **142**, 8 (1984).

[8] M. Misra, M. Satpathy, and L. Satpathy, J. Phys. G **14**, 1115 (1988).

[9] L. Satpathy, M. Mishra, A. Das, and M. Satpathy, Phys. Lett. B **237**, 181 (1990).

[10] A. Das, M. Mishra, M. Satpathy, and L. Satpathy, J. Phys. G **19**, 319 (1993).

[11] A. Das, M. Satpathy, and L. Satpathy, J. Phys. G **20**, 189 (1994).

[12] D. H. E. Gross, L. Satpathy, Meng Ta-chung, and M. Satpathy, Z. Phys. A **309**, 41 (1982).

[13] S. Das Gupta and A. Z. Mekjian, Phys. Rep. **72**, 131 (1981).

[14] H. Fuchs and K. Möhring, Rep. Prog. Phys. **57**, 231 (1994).

[15] C. B. Fulmer, J. B. Ball, R. L. Ferguson, R. L. Robinson, and J. R. Wu, Phys. Lett B **100**, 305 (1981).

[16] T. Li, W. Bauer, D. Craig, M. Cronqvist, S. Hannuschke, R. Lacey, W. J. Liope, T. Reposeur, A. M. Vander Molen, G. D. Westfall, W. K. Wilson, J. S. Winfield, J. Yee, S. J. Yennello, A. Nadasen, R. S. Tickle, and E. Norbeck, Phys. Rev. Lett. **70**, 1924 (1993).

[17] H. H. Heckman, D. E. Griener, P. J. Lindstorm, and H. Shwe, Phys. Rev. C **17**, 1735 (1978).

[18] Jicai Pan and Subal Das Gupta, Phys. Lett. B **344**, 29 (1995).